EurJOC European Journal of Organic Chemistry

FULL PAPER

DOI: 10.1002/ejoc.201500461

Synthesis and Optical Properties of a Series of Green-Light-Emitting 2-(4-Phenylquinolin-2-yl)phenol–BF_2 Complexes (Boroquinols)

Umamahesh Balijapalli[a] and Sathiyanarayanan Kulathu Iyer*[a]

Keywords: Dyes/Pigments / Boron / Fluorescence / Luminescence / Redox chemistry

A series of 2-(4-phenylquinolin-2-yl)phenol derivatives were efficiently synthesized and complexed with boron trifluoride to give fluorescent organoboron complexes. All the synthesized compounds were characterized by ^1H, ^{13}C, ^{11}B, ^{19}F NMR, FTIR, and HRMS analyses, and single-crystal structures of representative compounds were determined to examine the conformations of these compounds. The electronic properties of 2-(4-phenylquinolin-2-yl)phenol–BF_2 complexes were studied by absorption and fluorescence spectroscopy and the complexes were found to be highly emissive in the solid state. The electrochemical properties of boroquinols were measured by using cyclic voltammetry (CV) in acetonitrile with 0.1 M tetrabutyl ammonium hexafluorophosphate as a supporting electrolyte and the LUMO values of boroquinols were calculated to range from –2.64 to –3.46 eV, with HOMO values of –5.32 to –6.10 eV.

Introduction

Luminescent organic and organometallic compounds have attracted much interest because of their potential applications as biomolecular labels, molecular probes and switches, solar cells, laser dyes, photovoltaics, and organic light-emitting diode (OLEDs).[1] Among the various types of luminescent compounds, boron complexes based on N- and O-donor ligands have received particular attention because they exhibit excellent photophysical properties such as thermal, photo and chemical stability and high fluorescence quantum yield.[2] In particular, four-coordinate fluorescent organoboron complexes (FOBCs) constitute particularly elegant fluorescent dyes and they serve as efficient emitters in OLEDs. Several classes of four-coordinate boron chromophores including *N*,*O*-, *N*,*N*-, and *N*,*C*-chelate π-systems have been synthesized.[3] The four-coordinate boron molecules with four-, five- and six-membered ring fused skeletons have recently been produced as bright emitting materials with blue, green, and yellow emission colors.[4] FOBCs such as azobenzene, diketone, pyridomethene, pyrromethene, subphthalocyanine, subporphyrin, and others have been reported.[5] Specifically, boron-dipyrromethene (BODIPY) is well known to exhibit not only excellent optical properties such as sharp and narrow absorption and emission spectra, high photo and chemical stability, and good solubility, but it also plays a significant role in many fields including biomolecular probes and optoelectronics.[6] Moreover, there is the possibility of modulating the emission wavelength of such compounds by introducing functional groups and/or extending the conjugation around the fluorescent core.[7]

Most BODIPY dyes, however, possess very small Stokes shift values (400–600 cm^{-1}) because of their molecular rigidity with minimal differences between the ground- and excited-state structures.[8] Such small Stokes shifts make it impossible for optical filters to cut off the excitation light, which makes it difficult to identify the fluorescence signal over the noise in a bioassay. It also results in the reabsorption of its own fluorescence, thereby quenching the fluorescence intensity..[9] Furthermore, most BODIPY dyes possess intermolecular interactions due to their high planarity, which increases the concentration-quenching effect in the solid state. Thus, these molecules exhibit almost no fluorescence in the solid state, which may explain why BODIPYs are rarely applied as electroluminescence materials.[10] Although some efforts have been made to induce larger Stokes shifts in BODIPY derivatives, the major problem has been the loss of energy through nonradiative decay of the excited fluorophores.[11] Recently *N*-benzylideneaniline, benzoxazole, benzothiazole, pyridomethene, pyrazine, thiazole, naphthyridine, pyrazolyl aniline, indocarbazole, phenanthro imidazole, coumarin, iminocoumarin and isatin–phenylhydrazone–BF_2 complexes have been studied extensively as an analogue of BODIPY dyes.[12]

Thus, in a continuation of this quest, we attempted to explore a new class of four-coordinated quinoline-based boron complexes to substitute BODIPY derivatives as multifunctional fluorophores for broader applications with excellent emitting properties. In this paper, we outline the synthesis and fluorescence properties of new quinoline–boron complexes (boroquinols) that exhibit green fluores-

[a] Chemistry Division, School of Advanced sciences, Vellore Institute of Technology,
Vellore 632014, Tamilnadu, India
E-mail: sathiya_kuna@hotmail.com
https://www.sites.google.com/site/sathiyanarayananresearchgroup/

Supporting information for this article is available on the WWW under http://dx.doi.org/10.1002/ejoc.201500461.

cence both in solution and in the solid state with large Stokes shift (3688–10231 cm^{-1}). To our knowledge, there has only been one report describing related boroquinol complexes with photophysical properties and no detailed electrochemical studies were reported.[13] The main advantage of the current study was the introduction of the phenyl substituent on the quinoline, which should improve the solid-state emission properties by reducing π–π interaction between chromophores, and could be a handle for future derivatization.

Results and Discussion

Substituted 2-(4-phenylquinolin-2-yl)phenol (PQPs) derivatives were obtained by heating the corresponding aniline, salicylaldehyde, and phenylacetylene to reflux in nitromethane solution in the presence of iodine and cuprous oxide (Cu_2O), which gave moderate to good yields (Scheme 1). These compounds were very weakly fluorescent in solution because of an excited state intramolecular proton transfer (ESIPT) process. The reaction of the 2-(4-phenylquinolin-2-yl)phenol (PQPs) with boron trifluoro diethyl etherate ($BF_3{\cdot}OEt_2$) in the presence of triethylamine gave quinoline-containing BF_2 complexes (Scheme 1). The reaction was readily monitored by ^1H NMR spectroscopy because the phenolic OH signal of the 2-(4-phenylquinolin-2-yl)phenol at δ = 15.5 ppm disappeared progressively; this was further affirmed by ^{11}B and ^{19}F NMR spectroscopy. In addition, these compounds are strongly fluorescent in the solution state because of an intramolecular charge transfer (ICT) process. The quinoline structures and quinoline–boron complex structures were fully characterized and confirmed by ^1H, ^{13}C, ^{11}B, ^{19}F NMR, FTIR, HRMS, and X-ray crystallography. Details of the experimental procedures and

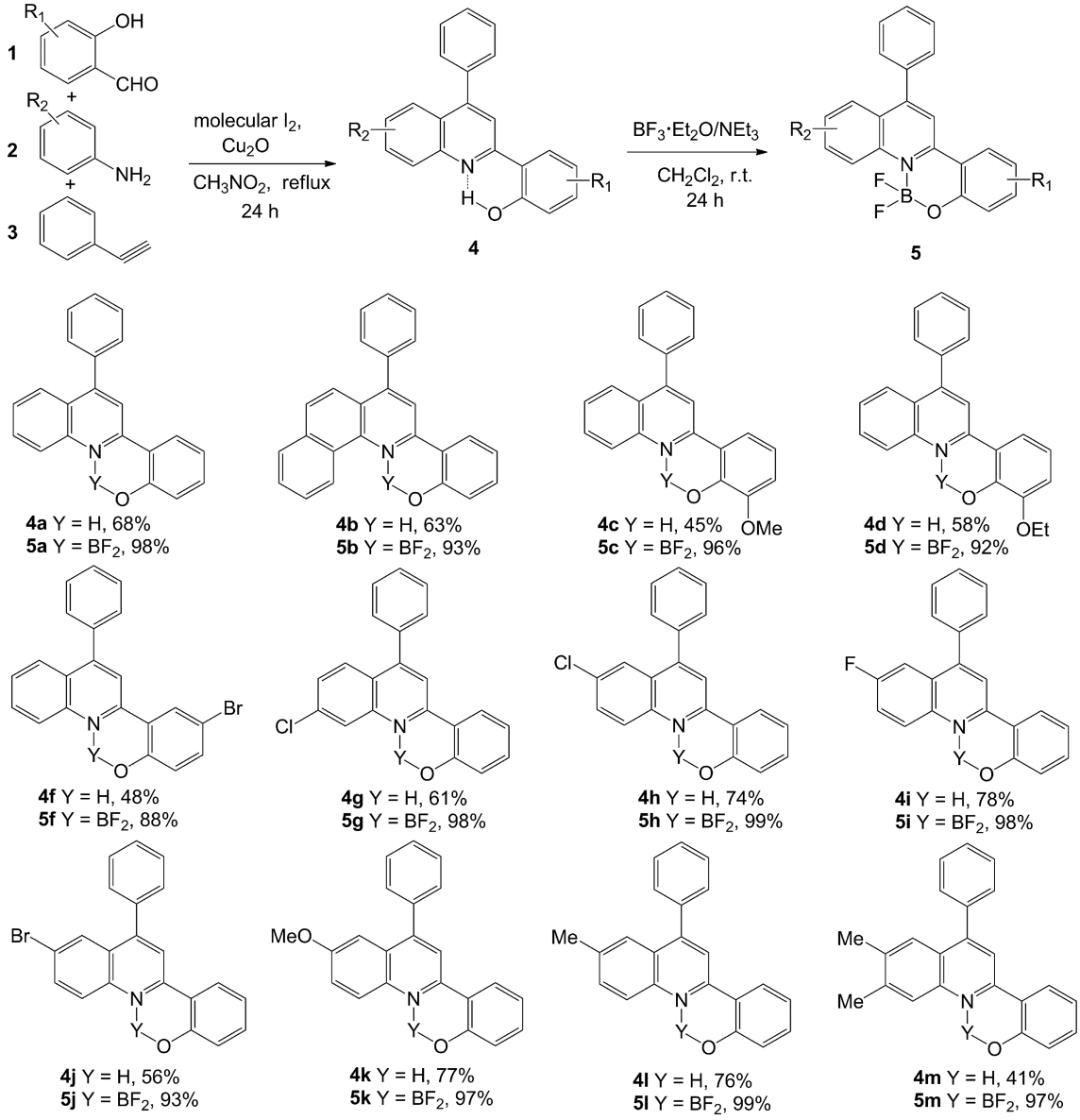

Scheme 1. Synthesis of substituted 2-(4-phenylquinolin-2-yl)phenol derivatives **4a**–**l** and their corresponding boron(III) complexes **5a**–**l**.

structural characterization data along with spectra are presented in the Supporting Information.

Furthermore, to explore the solid-state fluorescence properties of these compounds, X-ray crystallographic analysis was performed for compound **5h**. A single crystal of ligand **5h** that was suitable for X-ray diffraction studies was grown by slow evaporation from ethanol and tetrahydrofuran solutions at room temperature. ORTEP diagrams of boroquinol **5h** are given in Figure 1 (top and bottom). The complex crystallized as a triclinic system without solvation and the boron atom was coordinated in a tetrahedral geometry by nitrogen, oxygen, and two fluorine atoms with one F–B–F center. In the crystal structure of **5h**, the boron atom (B^1) lies –0.065(2) Å in the least square plane containing N^1, O^1, C^1, C^6, and C^7 atoms, and the ring has almost planar structure (see the Supporting Information, Figure S6). The central B-atom possessed B–F^1, B–F^2, B–N, B–O bond lengths of 1.378(2), 1.364(2), 1.607(2), and 1.410(2) Å, respectively, and bond angles around the B atom ranged from 106.8 to 111.35 Å [F^2–B^1–F^1 110.03(2), F^2–B^1–O^1 108.45(2), F^1–B^1–O^1 110.54(1), F^2–B^1–N^{1+} 109.63(1), F^1–B^1–N^1 106.83(1), O^1–B^1–N^1 111.35(1)]. The bond lengths and bond angles were similar to *N*,*O*-chelated BF_2 complexes. As depicted in Figure 1, the phenyl moiety at the C^9-atom exhibited distorted geometry from the planar quinoline complex. The molecule is essentially coplanar, and all portions except for the phenyl moiety at the C^9-atom and two F-atoms were located in the same plane, which suggests the formation of an extended π-conjugation system that is favorable for intramolecular charge transfer. The crystal structure of **5h** thus showed a π-conjugated framework exhibiting B–O interactions, which resulted in a

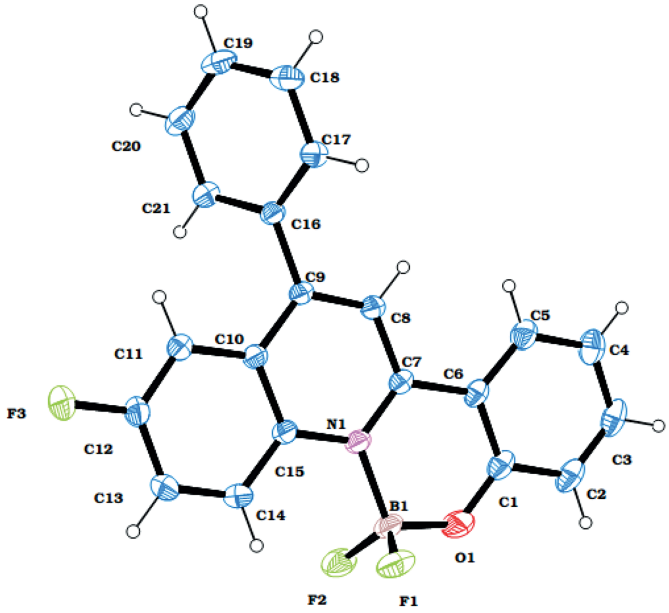

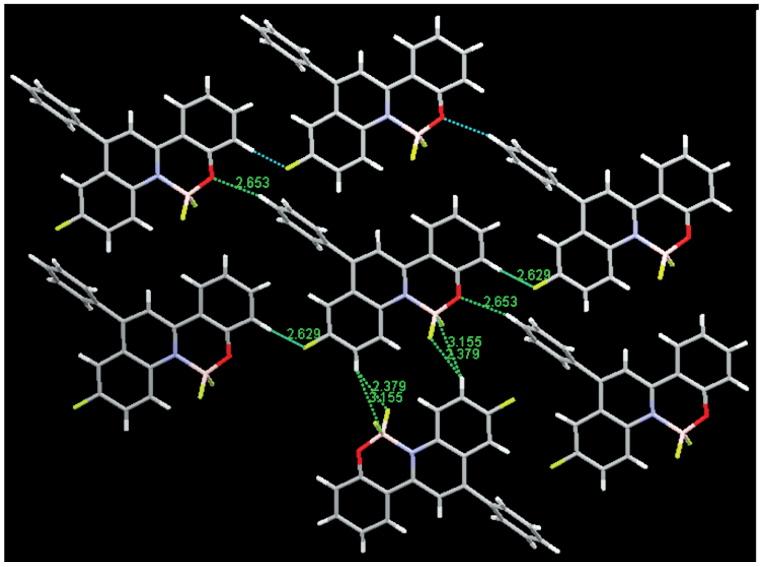

Figure 1. Top: ORTEP diagram for boroquinol **5h** (CCDC-1049309); bottom: intermolecular π-π interactions among the complexes of **5h**.

rigid molecular structure. As shown in Figure 1 (bottom), the molecules were arranged in a layer fashion and significant intermolecular CH–π, and π–π interactions were found to exist along the crystallographic axis direction with different intermolecular distance of CH–π···O (2.653 Å), CH–π···F (2.629 Å), CH–π···B (3.155 Å), and CH–π···F^2–B (2.379 Å). The intermolecular π–π interactions linked the neighboring molecules and hence resulted in the formation of network π–π interactions. The π–π interactions are known to cause fluorescence quenching in the solid state.[14] Surprisingly, despite the existence of π–π networks, the compounds exhibited strong fluorescence in the solid state.

The UV/Vis absorption and fluorescence spectra of **4a**–**l** were measured in chloroform and are shown in the Supporting Information (Figure S14–S15). The UV/Vis absorption spectra of **4a** showed two absorption peaks at 297 (weak) and 348 (strong) nm, which can be attributed to π→π* and hydrogen bonding between the phenolic OH and quinoline nitrogen atom respectively. The PQP ligands were weakly emissive but showed large Stokes shifts (Δ_{ss}) and high molar extinction coefficient values through an excited-state intramolecular proton transfer process; this is a characteristic feature of hydroxybenzoxazole family that was responsible for the large Stokes shifts.[12b] Indeed, the tautomerization in the excited state led to the keto form that is responsible for the lower energy emission. The absorption and emission data of PQP ligands are summarized in the Supporting Information (Table S1). The photophysical properties of the newly synthesized boroquinols **5a**–**l** were recorded in chloroform solvent as shown in the Supporting Information (Figure S16–S18) and the corresponding data are summarized in Table 1. The absorption and fluorescence spectra of ligands **4a** and **4b**, and corresponding complexes **5a** and **5b** in chloroform are shown in Figure 2.

The absorption spectra of complexes **5a**–**l** exhibited a major absorption band between 250 and 415 nm. UV/Vis absorption spectra of **5a** showed three absorption peaks at 288, 329, and 375 nm. The weak absorption peaks at 288, 319 nm and the strong absorption peak at 375 nm could be

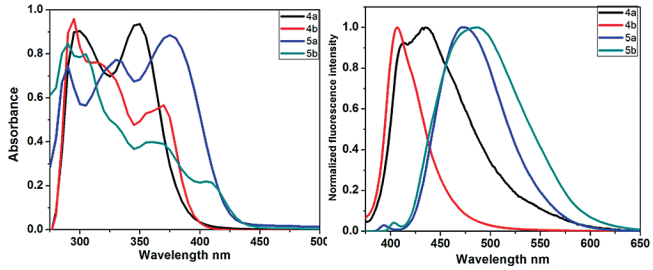

Figure 2. UV/Vis absorption (left) and fluorescence spectra (right) of **4a**, **4b**, **5a** and **5b** in chloroform measured at a concentration of 1×10^{-5} mol dm^3 of substrate at 25 °C.

attributed to π→π* transition and n→π* transition, respectively. Compound **5a** exhibited maximum absorption wavelength (λ_{max}) at 375 nm, which is a 10 nm bathochromic shifted compared with **5b** (365 nm). In addition to the strong absorption band at 291 nm, weak absorption bands were present at 365, 415 nm along with the vibrational peaks, and this could be attributed to π–π transitions present in **5b**. Although **4a** and **4b** exhibited very weak fluorescence in chloroform solvent, **5a** and **5b** showed enhanced bluish green fluorescence at 476 and 490 nm, respectively. The steady-state fluorescence spectrum of **5a** was observed at 476 nm with mirror image relationship to the lowest energy absorption band shown in Figure 3 and this is common for all the boroquinols (see the Supporting Information, Figure S2–S13). The emission spectra of boroquinols **5a**–**l** (see the Supporting Information, Figure S18) exhibited a major emission between 467 and 538 nm with large Stokes shifts in the range 3688–10231 cm^{-1}. The λ_{max} of **5c** (531 nm) and **5d** (538 nm) were redshifted by 55 and 62 nm, respectively, compared with that of **5a** (476 nm). Unlike the low stokes shift values in BODIPYs, higher stokes shift values were observed for these boroquinols in the range of 3688–10231 cm^{-1}. Larger Stokes shift values (Δ_{ss}) observed for **5c** (9543 cm^{-1}) and **5d** (10231 cm^{-1}) were higher than that of **5a** (5658 cm^{-1}) assigned to increased ICT character. This large Stokes shift may be attributed to the increased electron density as a result of the donating

Table 1. Optical properties of quinoline–boron complexes in chloroform.

5	Solution state[a] λ_{abs} [nm] (ε 10^4 M^{-1} cm^{-1})	λ_{em} [nm]	Solid state λ_{em} [nm]	Δss [cm^{-1}]	Φ_{fl}[b]	τ [ns][c]	K_r [10^8 s^{-1}]	K_{nr} [10^8 s^{-1}]
5a	288(1.27), 329(1.32), 375(1.5)	476	484, 597	5658	0.09	4.94	0.18	1.82
5b	289(1.5), 365(0.7), 415(0.38)	490	470	3688	0.22	4.77	0.46	1.63
5c	283(1.32), 348(1.57)	531	535	9543	< 0.01	1.45	0.07	6.93
5d	284(1.21), 347(1.43)	538	556	10231	< 0.01	2.0	0.05	4.95
5e	250(1.16), 297(1.62),351(1.72)	486	502, 587	7913	< 0.01	1.07	0.09	8.91
5f	291(1.43), 376(1.33)	485	492	5977	0.08	4.99	0.16	1.84
5g	289(1.45), 334(1.05), 382(1.11)	484	493	5517	0.10	4.64	0.22	1.98
5h	288(1.56), 328(1.41), 378(1.37)	482	487	5708	0.12	2.75	0.44	3.22
5i	289(1.63), 338(1.13), 381(1.22)	484	492	5586	0.09	2.02	0.45	4.55
5j	352(2.42), 385(2.62)	467	510	4560	0.08	2.94	0.27	3.10
5k	291(1.18), 332(1.15), 376(1.44)	471	486	5290	0.09	4.01	0.22	2.22
5l	285(1.54), 375(1.64)	496	481	6505	0.03	2.15	0.14	4.52

[a] Measured in chloroform at a concentration of 1.0×10^{-5} mol dm^{-3} at 25 °C. [b] The fluorescence quantum yields (Φ_F) were estimated with quinine sulfate (Φ_F) 0.55 in 1 N H_2SO_4 solution as a standard, λ_{ex} = 366 nm. [c] Fluorescence lifetime measured in chloroform by exciting the sample with a 342 nm, 150 ps pulse using nano-LEDs.

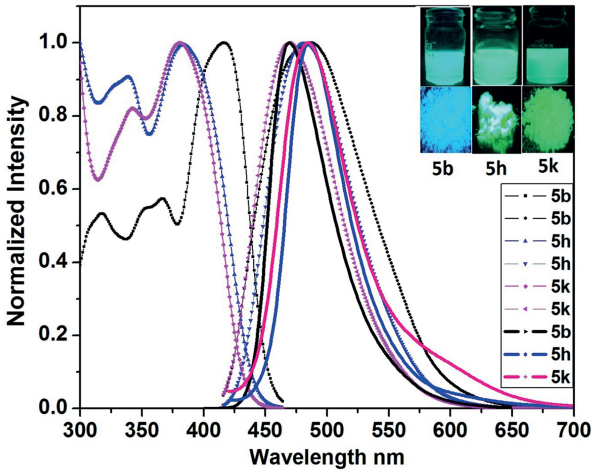

Figure 3. Excitation (dotted), luminescence (dotted) in chloroform and solid state luminescence (solid line) spectra of **5b** (black), **5h** (blue) and **5j** (pink). **Inset**. Solution and solid-state fluorescence images taken at 365 nm.

nature of methoxy and ethoxy groups present on the phenol ring of the boroquinol in the excited state. By increasing the electron density on the quinoline side by substituting methyl or methoxy groups in the *para*-position (boroquinol **5j**–**k**), λ_{max} of **5j** (467 nm) and **5k** (471 nm) were slightly blueshifted by 9 and 5 nm compared with that of **5a** (476 nm). Switching from electron-donating methyl/methoxy groups to F-, Cl-, Br- (boroquinol **5g**–**i**) shifted the emission bathochromically (484, 482, and 484 nm) by 8, 6 and 8 nm respectively to that of **5a**. Due to the larger Stokes shift that originated from internal charge transfer from the phenol to the quinolinium at the excited state, the overlap between the absorption and emission bands became minimal (Figure 2), which is a desirable characteristic for the dyes to be used in many fluorescence-based applications.[15] The solid-state emission spectra of boroquinols **5a**–**l** exhibited major emission maxima between 481 and 556 nm except for **5a** (484, 597 nm) and **5e** (502, 587 nm), which had two emission maxima, represented in Figure 3. In general, the solid-state emission maxima of the complexes were redshifted when compared with their emission maxima in solution except for **5b**, for which a 20 nm blueshift was observed. The broad shape of the emission band for boroquinols **5a**–**l**, the nonmirror symmetry with the absorption bands and a large Stokes shift (3688–10231 cm^{-1}) are suggestive of an intraligand charge transfer (ILCT) emissive state.

These dyes exhibited quantum yields in the range of 0.22–0.01 with good chemical and photochemical stability in apolar solvents. Compounds **5c**–**e** exhibited very low quantum yields, which was attributed the destabilization of the boroquinol through increased electron-density as a result of the substituents present on the phenolic ring of the complex. The absorption and fluorescence properties of **5a** and **5b** in various solvents were investigated are shown in the Supporting Information (Figure S20–S21). Generally, the absorbance maxima of **5a** were blueshifted in polar solvents when compared with nonpolar toluene and CH_2Cl_2. However, in the case of **5b**, a redshifted absorption was observed in CH_2Cl_2. The fluorescence maxima of **5a** were significantly affected by solvent polarity; in particular, a redshift in emission was observed in **5a** upon moving from toluene to dimethyl sulfoxide (DMSO), with the exception of MeOH in which a 82 nm blueshift was observed. For compound **5b**, the fluorescence maxima were blueshifted upon moving from toluene to DMSO. Notably, dissolving these complexes in polar solvents such as MeOH, CH_3CN, and DMSO led to the progressive decomplexation of boron, as shown by the recovery of the typical ESIPT emission of the PQP ligand.

To gain information on the excited-state processes, the fluorescence lifetime of boroquinols were measured by the time correlated single photon counting method by exciting the sample with a 342 nm, 150 ps pulse using nano-LEDs. The decay profiles of boroquinols derivatives **5a**–**d** in chloroform are given in Figure 4. The decay profiles can be fitted with a single exponential function. The lifetime data are summarized in Table 1. The fluorescence lifetime of **5a** and **5b** were measured to be 4.94 and 4.77 ns, respectively. Generally, the fluorescence lifetimes of phenolic-substituted compounds are shorter than that of the unsubstituted compound **5a**. However, the shorter lifetime values were measured for **5h**, **5i**, and **5j** (2.75, 2.02, and 2.94 ns, respectively) when compared with **5a**, even though they possess different functional groups such as halogens (F, Br) or methoxy substituents, respectively, present on the boroquinol.

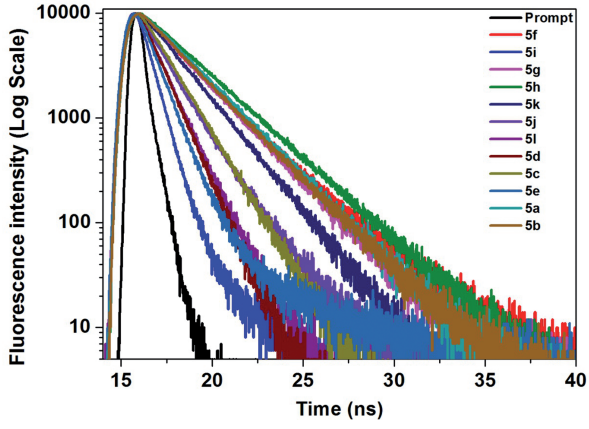

Figure 4. The lifetime decay profiles of boroquinols derivatives **5a**–**d** in chloroform.

The electrochemical properties of boroquinols were measured by using cyclic voltammetry (CV) in acetonitrile solvent with 0.1 M tetrabutylammonium hexafluorophosphate as a supporting electrolyte; a representative CV is illustrated in Figure 5. The first oxidation and reduction potential of all the compounds are summarized in Table 2. The HOMO and LUMO levels were readily estimated from the onset oxidation (E_{ox}) and onset reduction potentials (E_{red}) by using the equations $E_{HOMO} = -(E_{ox} + 4.8)$ eV and $E_{LUMO} = -(E_{red} + 4.8)$ eV and the data outlined in Table 2. All the

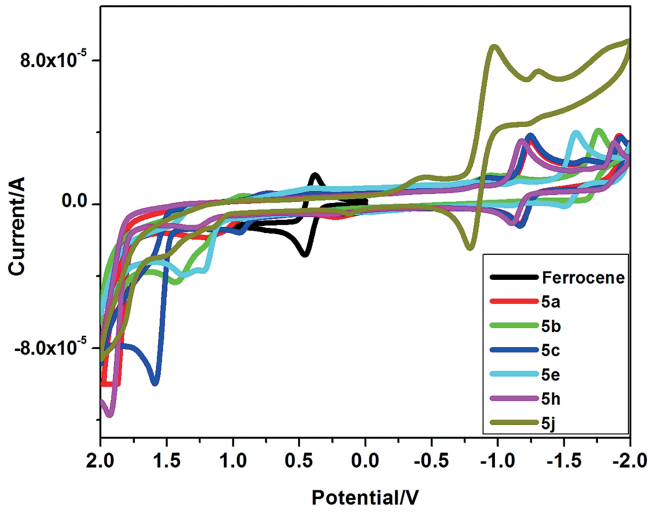

Figure 5. Cyclic voltammograms of compound **5a**–**c**, **5e**, **5h**, and **5j** measured at a scan rate of 100 mV s^{-1} in acetonitrile solvent using glassy carbon as working electrode and 0.1 M TBAHFP as supporting electrolyte.

Table 2. Electrochemical data of boroquinols **5a**–**l**.

5	$E^{1/2}_{ox}$ [V][a]	$E^{1/2}_{red}$ [V][a]	E_{HOMO} [eV][b]	E_{LUMO} [eV][b]	E_g [eV][c]
5a	n.d./1.19	–1.20	–5.99	–3.60	2.39
5b	n.d./1.44	–1.70	–6.24	–3.10	3.14
5c	n.d./0.95	–1.20	–5.75	–3.60	2.15
5d	n.d./0.94	–1.20	–5.74	–3.60	2.14
5e	n.d./1.23	–1.54	–6.03	–3.26	2.77
5f	n.d./1.48	–1.13	–6.28	–3.67	2.61
5g	n.d./1.28	–1.11	–6.08	–3.69	2.39
5h	n.d./1.29	–1.14	–6.09	–3.66	2.43
5i	n.d./1.35	–1.10	–6.15	–3.70	2.45
5j	n.d./1.52	–0.88	–6.32	–3.92	2.40
5k	n.d./1.68	–0.86	–6.48	–3.94	2.54
5l	n.d./1.14	–0.88	–5.94	–3.92	2.02

[a] The redox potential of compounds obtained from cyclic voltammetry using glassy carbon as working electrode with reference to the Fc/Fc$^+$ couple; 0.1 M tetrabutylmmonium hexafluorophosphate was used as supporting electrolyte; n.d.: not determined. [b] $E_{HOMO/LUMO}$ HOMO and LUMO energy levels calculated from the redox potentials using the equation $E_{HOMO} = E_{ox} + 4.8$ and $E_{LUMO} = E_{red} + 4.8$. [c] E_g = electrochemical HOMO–LUMO energy gap.

compounds show irreversible anodic redox process in the potential ranges of 0.94 to 1.68 V vs. ferrocenium/ferrocene redox couple. The oxidation process of boroquinols could be attributed to the irreversible oxidation of phenolic group of quinolines. In contrast, the reversible cathodic redox process spread over a larger potential range of –0.86 to –1.70 V and this is characteristic of the substituents present on the quinoline ring. Given that the electron-donating/withdrawing groups were substituted on the quinoline moiety, this significantly enhanced the electrochemical reduction behavior of the species. Complexes **5b** showed more negatively shifted reduction waves compared with complex **5a**, which is indicative of the enhancement of π-conjugation when replacing the phenyl group by a naphthyl group. However, multiple redox waves, i.e., single two-electron process, is observed in acetonitrile for few compounds. This was attributed to a negative shift of the redox potential for the first reduction because of the preferential solvation of more positively charged species by acetonitrile. In addition, the single two-electron process was split into two one-electron processes because of the large increase in ΔEp for the second reduction relative to that of the first reduction and to the small difference in the redox potentials. A greater reduction potential of –1.70 V was observed for **5b**. On the basis of the reduction potentials, the lowest unoccupied molecular orbital (LUMO) energy levels were calculated to be in the range of –3.10 to –3.94 eV. Moreover, the reduction potentials of **5a**–**l** shifted positively in the range of 0.80 and 1.64 V compared with that of tris(8-hydroxyquinolinato)-aluminium (Alq_3) (*E*pc = –2.3 V), which is one of the most widely used electron-transporting materials. This confirmed the high electron-accepting ability of these boron complexes.[4a] The HOMO values were calculated to be in the range –5.74 to –6.48 eV, which are similar to that of Alq_3 (–5.7 eV).[16]

Conclusions

We have developed quinoline-based boron complexes by the reaction of 2-(4-phenylquinolin-2-yl)phenol with boron trifluoride and investigated its optical properties. Significant features such as strong green fluorescence in the solid-state and moderate fluorescence in solution, unusually large Stokes shifts of 3688–10231 cm^{-1}, and lower LUMO and higher HOMO levels were observed. The fluorescence maximum and fluorescence quantum yields were in the range 467–538 nm and 0.01–0.22, respectively. Due to the existence of CH–π···O, CH–π···F, and CH–π···B networks, the compounds exhibited strong fluorescence in the solid state. The LUMO values of **5a**–**l** were calculated to be in the range –3.10 to –3.94 eV and HOMO values were –5.74 to –6.48 eV. These values are similar to that of electron-transporting material Alq_3 (*E*pc = –2.3 V, LUMO –3.0 eV, and HOMO –5.7 eV). These properties qualify these novel boroquinol complexes as not only multifunctional fluorophores but also as an alternative material that can be employed in sensing applications.

Experimental Section

General Information: All organic chemicals and solvents were purchased from Sigma–Aldrich, Merck, or Himedia. Purity of all the chemicals was greater than 99%. ^{1}H and ^{13}C NMR spectra were taken with a Bruker 300 MHz spectrometer using $CDCl_3$ or [D_6]-DMSO as the solvent with TMS as internal standard. Melting points were measured with a Guna capillary-based melting-point apparatus and were not corrected. HRMS values were obtained with a Joel GC Mate II GC-Mass Spectrometer. FTIR spectra of the synthesized organic compounds were recorded with a Jasco-4100 spectrometer. UV/Vis spectra were taken with a Hitachi U-2910 spectrophotometer. Fluorescence spectra in solution and solid were measured with a Hitachi F-7000 fluorescence spectrometer.

The fluorescence quantum yields (ΦF) were measured with quinine sulfate (ΦF 0.55 in 1 N H_2SO_4 solution) as standard, λ_{ex} = 366 nm. Analytical thin-layer chromatography (TLC) was performed on precoated plates (Merck, silica gel 60 F254). Silica gel (60–120 mesh) was used for column chromatography. Single-crystal X-ray diffraction data were recorded with a Bruker Kappa APEXII. The structures were solved by direct methods.

General Procedure for the Preparation of 4a–l: A mixture of substituted salicylaldehyde **1** (10 mmol) and substituted aromatic amine **2** (10 mmol) was stirred in nitromethane at room temperature for 10 min. After addition of 10 mol-% anhydrous iodine and 20 mol-% of Cu_2O, phenyl acetylene **3** (10 mmol) was added and the reaction mixture was heated to reflux for 24 h. Upon completion of the reaction (monitored by TLC analysis), the reaction mixture was cooled and diluted with saturated $NaHCO_3$ (80 mL). The mixture was extracted with ethyl acetate (3× 20 mL) and the combined organic extract was washed with brine and dried with (Na_2SO_4). The solvent was distilled off and the resulting product was purified by column chromatography over silica gel (60–120 mesh; *n*-hexane/ethyl acetate, 9:1) to give the product **4a**–**m**.

2-(4-Phenylquinolin-2-yl)phenol (4a): Yellow solid; m.p. 153–155 °C. IR (KBr): $\tilde{\nu}$ = 3263, 3088, 3057, 3030, 2917, 2876, 2331, 1737, 1585, 1467, 1433, 1398, 1274, 1213, 1120, 893, 752, 698, 675, 663, 646 cm^{-1}. ^1H NMR (400 MHz, $CDCl_3$): δ = 6.95–6.91 (t, J = 8.0 Hz, 1 H), 7.10–7.08 (t, J = 8.0 Hz, 1 H), 7.37–7.33 (t, J = 8.0 Hz, 1 H), 7.50–7.46 (t, J = 8.0 Hz, 1 H), 7.58–7.51 (m, 5 H), 7.75–7.71 (t, J = 8.0 Hz, 1 H), 7.88–7.86 (d, J = 8.0 Hz, 1 H), 7.95–7.94 (d, J = 4.0 Hz, 2 H), 7.50–7.46 (t, J = 8.0 Hz, 1 H), 8.09–8.07 (d, J = 8.0 Hz, 1 H), 15.29 (s, 1 H) ppm. ^{13}C NMR (100 MHz, $CDCl_3$): δ = 117.5, 118.6, 118.7, 118.9, 121.2, 125.3, 125.8, 126.7, 126.9, 126.9, 127.9, 128.7, 128.7, 129.4, 129.4, 130.3, 132.0, 137.9, 145.2, 150.2, 157.4, 161.1 ppm. HRMS: *m*/*z* calcd. for $C_{21}H_{15}NO$ [M^+] 297.1154; found 297.1150.

2-(4-Phenylbenzo[*h*]quinolin-2-yl)phenol (4b): Yellow solid; m.p. 180–182 °C. IR (KBr): $\tilde{\nu}$ = 3256, 3092, 3057, 3013, 2976, 2337, 2328, 2297, 1944, 1815, 1705, 1583, 1492, 1365, 1296, 1280, 1215, 1195, 1068, 876, 829, 704, 628 cm^{-1}. ^1H NMR (400 MHz, $CDCl_3$): δ = 6.96–6.92 (t, J = 8.0 Hz, 1 H), 7.15–7.13 (d, J = 8.0 Hz, 1 H), 7.39–7.35 (t, J = 8.0 Hz, 1 H), 7.55–7.53 (m, 5 H), 7.78–7.68 (m, 4 H), 7.89–7.87 (d, J = 8.0 Hz, 1 H), 7.97–7.95 (d, J = 8.0 Hz, 1 H), 8.05 (s, 1 H), 8.98–8.96 (d, J = 8.0 Hz, 1 H), 15.54 (s, 1 H) ppm. ^{13}C NMR (100 MHz, $CDCl_3$): δ = 118.3, 118.5, 118.9, 119.2, 122.7, 123.2, 124.1, 126.9, 127.7, 128.2, 128.7, 128.7, 128.7, 129.6, 129.7, 131.9, 133.8, 138.2, 143.7, 150.3, 155.8, 160.6 ppm. HRMS: *m*/*z* calcd. for $C_{25}H_{17}NO$ [M^+] 347.1310; found 347.1312.

2-Methoxy-6-(4-phenylquinolin-2-yl)phenol (4c): Yellow solid; m.p. 164–166 °C. IR (KBr): $\tilde{\nu}$ = 3250, 3087, 3053, 2985, 2945, 2825, 2336, 1741, 1591, 1550, 1431, 1363, 1240, 1049, 902, 758, 705, 601 cm^{-1}. ^1H NMR (400 MHz, $CDCl_3$): δ = 3.97 (s, 3 H), 6.90–6.86 (t, J = 8.0 Hz, 1 H), 6.99–6.97 (d, J = 8.0 Hz, 1 H), 7.52–7.48 (t, J = 8.0 Hz, 1 H), 7.59–7.56 (m, 6 H), 7.77–7.73 (t, J = 8.0 Hz, 1 H), 7.89–7.87 (d, J = 8.0 Hz, 1 H), 7.96 (s, 1 H), 8.09–8.07 (d, J = 8.0 Hz, 1 H), 15.88 (s, 1 H) ppm. ^{13}C NMR (100 MHz, $CDCl_3$): δ = 56.1, 113.3, 117.8, 118.6, 118.8, 125.3, 125.8, 126.7, 127.8, 128.7, 128.7, 129.4, 130.4, 137.9, 145.0, 149.5, 150.2, 151.6, 157.60 ppm. HRMS: *m*/*z* calcd. for $C_{22}H_{17}NO_2$ [M^+] 327.1259; found 327.1260.

2-Ethoxy-6-(4-phenylquinolin-2-yl)phenol (4d): Yellow solid; m.p. 157–159 °C. IR (KBr): $\tilde{\nu}$ = 3258, 3099, 3053, 2981, 2904, 2872, 2337, 1717, 1593, 1548, 1462, 1440, 1357, 1238, 1049, 1031, 902, 875, 858, 769, 702, 574 cm^{-1}. ^1H NMR (400 MHz, $CDCl_3$): δ = 1.57–1.53 (t, J = 8.0 Hz, 3 H), 4.20–4.14 (q, J = 8.0 Hz, 2 H, 3 H), 6.87–6.83 (t, J = 8.0 Hz, 1 H), 6.98–6.96 (d, J = 8.0 Hz, 1 H), 7.50–7.46 (t, J = 8.0 Hz, 1 H), 7.56–7.55 (m, 6 H), 7.75–7.71 (t, J = 8.0 Hz, 1 H), 7.88–7.86 (d, J = 8.0 Hz, 1 H), 7.95 (s, 1 H), 8.07–8.05 (d, J = 8.0 Hz, 1 H), 15.94 (s, 1 H) ppm. ^{13}C NMR (100 MHz, $CDCl_3$): δ = 15.0, 64.4, 114.6, 117.8, 118.6, 118.8, 125.3, 125.8, 126.7, 127.7, 128.7, 128.7, 129.4, 130.4, 137.9, 145.0, 148.8, 150.1, 151.7, 157.6 ppm. HRMS: *m*/*z* calcd. for $C_{23}H_{19}NO_2$ [M^+] 341.1416; found 341.1416.

4-Bromo-2-(4-phenylquinolin-2-yl)phenol (4e): Yellow solid; m.p. 184–186 °C. IR (KBr): $\tilde{\nu}$ = 3267, 3091, 3041, 3011, 2987, 2335, 1737, 1579, 1489, 1467, 1392, 1304, 1255, 1207, 1182, 1085, 975, 883, 812, 705, 680, 628, 597 cm^{-1}. ^1H NMR (400 MHz, $CDCl_3$): δ = 6.99–6.97 (d, J = 8.0 Hz, 1 H), 7.43–7.40 (dd, J = 16.0, 4.0 Hz, 1 H), 7.60–7.49 (m, 6 H), 7.77–7.73 (t, J = 8.0 Hz, 1 H), 7.90–7.88 (d, J = 8.0 Hz, 2 H), 8.04 (s, 1 H), 8.09–8.07 (d, J = 8.0 Hz, 1 H), 15.34 (s, 1 H) ppm. ^{13}C NMR (100 MHz, $CDCl_3$): δ = 110.4, 117.3, 120.5, 125.5, 125.9, 127.0, 127.9, 128.8, 128.9, 129.4, 129.4, 130.5, 134.5, 137.6, 145.1, 150.6, 156.0, 160.2 ppm. HRMS: *m*/*z* calcd. for $C_{21}H_{14}BrNO$ [M^+] 375.0259; found 375.0264.

2-(7-Chloro-4-phenylquinolin-2-yl)phenol (4f): Yellow solid; m.p. 140–142 °C. IR (KBr): $\tilde{\nu}$ = 3270, 3096, 3057, 2939, 2871, 2331, 1726, 1573, 1544, 1487, 1460, 1415, 1371, 1296, 1278, 1199, 1156, 1153, 1076, 981, 877, 821, 737, 626 cm^{-1}. ^1H NMR (400 MHz, $CDCl_3$): δ = 6.97–6.93 (q, J = 4.0 Hz, 1 H), 7.13–7.11 (d, J = 8.0 Hz, 1 H), 7.67–7.28 (m, 8 H), 7.84–7.82 (d, J = 8.0 Hz, 1 H), 7.96–7.91 (m, 2 H), 8.10–8.04 (m, 2 H), 14.82 (s, 1 H) ppm. ^{13}C NMR (100 MHz, $CDCl_3$): δ = 117.7, 118.3, 118.9, 121.2, 123.0, 123.7, 126.9, 127.5, 127.7, 127.8, 128.0, 128.8, 129.0, 129.9, 131.2, 132.4, 132.5, 136.3, 137.4, 140.7, 145.8, 146.9, 149.8, 150.1, 157.1, 158.5, 161.1 ppm. HRMS: *m*/*z* calcd. for $C_{21}H_{14}ClNO$ [M^+] 331.0764; found 337.0767.

2-(6-Chloro-4-phenylquinolin-2-yl)phenol (4g): Yellow solid; m.p. 156–158 °C. IR (KBr): $\tilde{\nu}$ = 3263, 3091, 3059, 3026, 2920, 2848, 2397, 2343, 1764, 1743, 1587, 1485, 1417, 1352, 1298, 1274, 1124, 1072, 869, 819, 738, 700, 684, 617 cm^{-1}. ^1H NMR (400 MHz, $CDCl_3$): δ = 6.98–6.94 (t, J = 8.0 Hz, 1 H), 7.13–7.11 (d, J = 8.0 Hz, 1 H), 7.42–7.38 (t, J = 8.0 Hz, 1 H), 7.64–7.55 (m, 5 H), 7.71–7.69 (d, J = 8.0 Hz, 1 H), 7.87–7.86 (d, J = 8.0 Hz, 1 H), 7.95–7.94 (d, J = 4.0 Hz, 1 H), 7.99 (s, 1 H), 8.05–8.03 (d, J = 8.0 Hz, 1 H), 14.90 (s, 1 H) ppm. ^{13}C NMR (100 MHz, $CDCl_3$): δ = 118.4, 118.7, 118.9, 119.2, 122.4, 124.7, 126.0, 127.0, 128.9, 129.0, 129.3, 129.5, 131.2, 132.3, 132.6, 133.4, 137.2, 143.7, 149.4, 157.7, 161.0, 162.9 ppm. HRMS: *m*/*z* calcd. for $C_{21}H_{14}ClNO$ [M^+] 331.0764; found 337.0763.

2-(6-Fluoro-4-phenylquinolin-2-yl)phenol (4h): Yellow solid; m.p. 167–169 °C. IR (KBr): $\tilde{\nu}$ = 3270, 3091, 3059, 2991, 2971, 2351, 2330, 1726, 1624, 1587, 1550, 1508, 1494, 1425, 1382, 1355, 1251, 1195, 1109, 925, 873, 746, 702, 655 cm^{-1}. ^1H NMR (400 MHz, $CDCl_3$): δ = 6.95–6.91 (t, J = 8.0 Hz, 1 H), 7.09–7.07 (d, J = 8.0 Hz, 1 H), 7.37–7.33 (t, J = 8.0 Hz, 1 H), 7.56–7.48 (m, 7 H), 7.93–7.91 (d, J = 8.0 Hz, 1 H), 7.96 (s, 1 H), 8.07 (s, 1 H), 14.88 (s, 1 H) ppm. ^{13}C NMR (100 MHz, $CDCl_3$): δ = 109.4, 109.7, 118.2, 118.6, 118.8, 118.8, 120.2, 120.4, 126.1, 126.2, 126.9, 128.9, 129.0, 129.2, 130.3, 130.4, 132.1, 137.4, 142.3, 149.6, 149.7, 156.9, 156.9, 159.4, 160.8, 161.9 ppm. HRMS: *m*/*z* calcd. for $C_{21}H_{14}FNO$ [M^+] 315.1059; found 315.1061.

2-(6-Bromo-4-phenylquinolin-2-yl)phenol (4i): Yellow solid; m.p. 166–168 °C. IR (KBr): $\tilde{\nu}$ = 3280, 3092, 3057, 3028, 2669, 2397, 2330, 1957, 1851, 1737, 1610, 1583, 1543, 1500, 1485, 1369, 1350, 1294, 1244, 1120, 1039, 871, 823, 746, 700, 669, 630 cm^{-1}. ^1H NMR (400 MHz, $CDCl_3$): δ = 6.99–6.95 (t, J = 8.0 Hz, 1 H), 7.13–7.11 (d, J = 8.0 Hz, 1 H), 7.42–7.38 (t, J = 8.0 Hz, 1 H), 7.65–7.55 (m,

5 H), 7.85–7.83 (dd, *J* = 16.0, 4.0 Hz, 1 H), 7.98–7.96 (d, *J* = 4.0 Hz, 2 H), 8.00 (s, 1 H), 8.04–8.03 (d, *J* = 4.0 Hz, 1 H), 14.91 (s, 1 H) ppm. ^{13}C NMR (100 MHz, $CDCl_3$): δ = 117.3, 118.4, 118.7, 118.9, 120.7, 122.8, 126.5, 127.0, 128.0, 128.9, 129.0, 129.3, 129.6, 132.3, 132.5, 133.7, 137.2, 144.0, 149.3, 157.8, 161.0, 161.1, 163.0 ppm. HRMS: *m*/*z* calcd. for $C_{21}H_{14}BrNO$ [M^+] 375.0259; found 375.0259.

2-(6-Methoxy-4-phenylquinolin-2-yl)phenol (4j): Yellow solid; m.p. 144–146 °C. IR (KBr): $\tilde{\nu}$ = 3266, 3088, 3043, 2999, 2943, 2331, 1778, 1620, 1585, 1543, 1506, 1494, 1386, 1267, 1215, 1120, 1029, 906, 887, 754, 698, 624, 590 cm^{-1}. ^{1}H NMR (400 MHz, $CDCl_3$): δ = 3.80 (s, 3 H), 6.94–6.90 (t, *J* = 8.0 Hz, 1 H), 7.09–7.07 (d, *J* = 8.0 Hz, 1 H), 7.17–7.16 (d, *J* = 4.0 Hz, 1 H), 7.35–7.31 (t, *J* = 8.0 Hz, 1 H), 7.42–7.38 (dd, *J* = 16.0, 4.0 Hz, 1 H), 7.57–7.53 (m, 5 H), 7.91 (s, 1 H), 7.93–7.92 (d, *J* = 4.0 Hz, 1 H), 8.01–7.99 (d, *J* = 8.0 Hz, 1 H), 15.13 (s, 1 H) ppm. ^{13}C NMR (100 MHz, $CDCl_3$): δ = 55.5, 104.2, 117.9, 118.5, 118.7, 119.1, 122.4, 126.3, 126.6, 128.7, 128.8, 129.2, 129.4, 131.5, 138.2, 141.1, 148.8, 155.1, 158.1, 160.7 ppm. HRMS: *m*/*z* calcd. for $C_{22}H_{17}NO_2$ [M^+] 327.1259; found 327.1259.

2-(6-Methyl-4-phenylquinolin-2-yl)phenol (4k): Yellow solid; m.p. 168–170 °C. IR (KBr): $\tilde{\nu}$ = 3250, 3089, 3047, 2926, 2858, 2330, 1741, 1583, 1546, 1490, 1355, 1246, 1124, 1076, 962, 871, 752, 744, 705, 594 cm^{-1}. ^{1}H NMR (400 MHz, $CDCl_3$): δ = 2.46 (s, 3 H), 6.94–6.90 (t, *J* = 8.0 Hz, 1 H), 7.09–7.07 (d, *J* = 8.0 Hz, 1 H), 7.36–7.32 (t, *J* = 4.0 Hz, 1 H), 7.57–7.53 (m, 6 H), 7.61 (s, 1 H), 7.91 (s, 1 H), 7.94–7.92 (d, *J* = 4.0 Hz, 1 H), 7.99–7.97 (d, *J* = 8.0 Hz, 1 H), 15.30 (s, 1 H) ppm. ^{13}C NMR (100 MHz, $CDCl_3$): δ = 21.8, 117.6, 118.5, 118.6, 119.1, 121.0, 124.6, 125.3, 126.8, 127.7, 128.6, 128.7, 129.4, 130.0, 131.8, 132.4, 136.8, 138.1, 143.7, 149.5, 156.5, 161.0, 161.7 ppm. HRMS: *m*/*z* calcd. for $C_{22}H_{17}NO$ [M^+] 311.1310; found 311.1316.

2-(5,7-Dimethyl-4-phenylquinolin-2-yl)phenol (4l): Yellow solid; m.p. 149–151 °C. IR (KBr): $\tilde{\nu}$ = 3290, 3142, 3057, 2978, 2861, 2328, 1735, 1597, 1494, 1411, 1381, 1363, 1300, 1222, 1153, 765, 756, 868, 659, 619, 588 cm^{-1}. ^{1}H NMR (400 MHz, $CDCl_3$): δ = 2.00 (s, 3 H), 2.54 (s, 3 H), 6.94–6.90 (t, *J* = 8.0 Hz, 1 H), 7.12–7.10 (d, *J* = 8.0 Hz, 1 H), 7.14 (s, 1 H), 7.40–7.28 (m, 3 H), 7.52–7.49 (m, 3 H), 7.79–7.77 (d, *J* = 8.0 Hz, 2 H), 7.92–7.90 (d, *J* = 8.0 Hz, 1 H), 15.44 (s, 1 H) ppm. ^{13}C NMR (100 MHz, $CDCl_3$): δ = 21.4, 24.1, 118.5, 118.5, 118.7, 118.7, 118.9, 122.8, 125.9, 126.8, 128.0, 128.0, 128.6, 131.8, 132.3, 135.3, 140.1, 142.4, 146.6, 150.4, 155.9, 161.2 ppm. HRMS: *m*/*z* calcd. for $C_{23}H_{19}NO$ [M^+] 325.1467; found 325.1469.

General Procedure for the Preparation of 5a–m: To a stirred solution of 2-(4-phenylquinolin-2-yl)phenol (1 mmol) in anhydrous dichloromethane (10 mL) at room temperature was added boron trifluoride–diethyl ether complex (2.5 mmol). A color change occurred or a precipitate appeared, revealing the formation of an intermediate adduct. Triethylamine (1.0 mmol) was then added to the solution, which was stirred at room temperature for 12–18 h. The course of the reaction was monitored by TLC analysis and, upon completion of the reaction, water was added to the solution. The solution was extracted with CH_2Cl_2 and the organic layer was washed with water and dried with $MgSO_4$. After concentration of solvent, the residue was purified by column chromatography with silica gel (CH_2Cl_2/*n*-hexane) to afford **5a** (52 mg, 97%) as a yellow solid.

6,6-Difluoro-13-phenyl-6*H*-benzo[5,6][1,3,2]oxazaborinino[3,4-*a*]-quinolin-5-ium-6-uide (5a): Yellow solid; m.p. 252–254 °C. IR (KBr): $\tilde{\nu}$ = 3055, 3026, 2922, 2852, 2333, 1717, 1604, 1550, 1267, 1101, 1073, 1002, 871, 837, 750, 742, 702, 663 cm^{-1}. ^{1}H NMR (400 MHz, $CDCl_3$): δ = 7.08–7.04 (t, *J* = 8.0 Hz, 1 H), 7.25–7.23 (d, *J* = 8.0 Hz, 1 H), 7.67–7.53 (m, 7 H), 7.99–7.91 (m, 3 H), 8.11 (s, 1 H), 9.07–9.05 (d, *J* = 8.0 Hz, 1 H) ppm. ^{13}C NMR (100 MHz, $CDCl_3$): δ = 117.5, 120.3, 120.4, 125.0, 126.6, 126.7, 126.8, 127.8, 129.0, 129.3, 129.9, 132.6, 135.5, 136.4, 151.9, 155.3, 156.3 ppm. ^{11}B NMR (128 MHz, $CDCl_3$): δ = 1.57 (s, BF_2) ppm. ^{19}F NMR (376 MHz, $CDCl_3$): δ = –(132.50–132.44) (2 F) ppm. HRMS: *m*/*z* calcd. for $C_{21}H_{14}BF_2NO$ [M^+] 345.1137; found 345.1131.

8,8-Difluoro-15-phenyl-8*H*-benzo[*h*]benzo[5,6][1,3,2]oxazaborinino-[3,4-*a*]quinolin-7-ium-8-uide (5b): Yellow solid; m.p. >300 °C. IR (KBr): $\tilde{\nu}$ = 3053, 3015, 2926, 2854, 2313, 1737, 1620, 1581, 1512, 1384, 1294, 1112, 1080, 958, 902, 869, 852, 756, 705, 675 cm^{-1}. ^{1}H NMR (400 MHz, $CDCl_3$): δ = 6.80–6.76 (t, *J* = 8.0 Hz, 1 H), 6.92–6.90 (d, *J* = 8.0 Hz, 1 H), 7.20–7.16 (t, *J* = 8.0 Hz, 1 H), 7.60–7.39 (m, 9 H), 7.77–7.75 (d, *J* = 8.0 Hz,1 H), 7.84–7.82 (d, *J* = 8.0 Hz,1 H), 7.92 (s, 1 H), 8.77–8.75 (d, *J* = 8.0 Hz, 1 H) ppm. ^{13}C NMR (100 MHz, $CDCl_3$): δ = 108.7, 118.8, 120.2, 122.5, 123.5, 126.5, 127.2, 128.1, 129.4, 129.7, 133.3, 136.8, 145.0, 154.3, 170.9 ppm. ^{11}B NMR (128 MHz, $CDCL_3$): δ = –1.16 (s, BF_2) ppm. ^{19}F NMR (376 MHz, $CDCl_3$): δ = –(148.45–148.38) (2 F) ppm. HRMS: *m*/*z* calcd. for $C_{25}H_{16}BF_2NO$ [M^+] 395.1293; found 395.1399.

6,6-Difluoro-8-methoxy-13-phenyl-6*H*-benzo[5,6][1,3,2]oxaza-borinino[3,4-*a*]quinolin-5-ium-6-uide (5c): Yellow solid; m.p. 247–249 °C. IR (KBr): $\tilde{\nu}$ = 3053, 3005, 2903, 2835, 2346, 1743, 1604, 1554, 1519, 1460, 1386, 1363, 1234, 1080, 1062, 1039, 935, 767, 727, 704 cm^{-1}. ^{1}H NMR (400 MHz, $CDCl_3$): δ = 3.99 (s, 3 H), 6.99–6.95 (t, *J* = 8.0 Hz, 1 H), 7.10–7.08 (d, *J* = 8.0 Hz, 1 H), 7.54–7.52 (d, *J* = 8.0 Hz, 1 H), 7.66–7.56 (m, 6 H), 7.97–7.89 (m, 2 H), 8.08 (s, 1 H), 9.09–9.07 (d, *J* = 8.0 Hz, 1 H) ppm. ^{13}C NMR (100 MHz, $CDCl_3$): δ = 56.2, 115.8, 118.0, 119.9, 125.0, 125.1, 126.1, 126.6, 126.8, 127.8, 128.9, 129.0, 129.3, 129.4, 129.8, 132.5, 136.4, 140.8, 150.2, 152.0, 155.2 ppm. ^{11}B NMR (128 MHz, $CDCl_3$): δ = 1.68 (s, BF_2) ppm. ^{19}F NMR (376 MHz, $CDCl_3$): δ = –(132.06–131.99) (2 F) ppm. HRMS: *m*/*z* calcd. for $C_{22}H_{16}BF_2NO_2$ [M^+] 375.1242; found 375.1249.

8-Ethoxy-6,6-difluoro-13-phenyl-6*H*-benzo[5,6][1,3,2]oxazaborinino-[3,4-*a*]quinolin-5-ium-6-uide (5d): Yellow solid; m.p. 240–242 °C. IR (KBr): $\tilde{\nu}$ = 3047, 2972, 2926, 2328, 1737, 1595, 1442, 1388, 1363, 1234, 1095, 1074, 1053, 962, 918, 873, 769, 723, 698 cm^{-1}. ^{1}H NMR (400 MHz, $CDCl_3$): δ = 1.57–1.53 (t, *J* = 8.0 Hz, 1 H), 4.26–4.20 (q, *J* = 8.0 Hz, 2 H), 6.98–6.94 (t, *J* = 8.0 Hz, 1 H), 7.12–7.10 (d, *J* = 8.0 Hz, 1 H), 7.55–7.53 (d, *J* = 8.0 Hz, 1 H), 7.66–7.57 (m, 6 H), 7.98–7.90 (m, 2 H), 8.08 (s, 1 H), 9.09–9.07 (d, *J* = 8.0 Hz, 1 H) ppm. ^{13}C NMR (100 MHz, $CDCl_3$): δ = 14.8, 65.0, 114.9, 117.9, 118.0, 118.1, 118.3, 119.9, 125.0, 125.9, 126.6, 126.8, 127.1, 127.8, 128.8, 129.0, 129.3, 129.4, 129.8, 132.5, 136.4, 152.1, 155.1 ppm. ^{11}B NMR (128 MHz, $CDCl_3$): δ = 1.67 (s, BF_2) ppm. ^{19}F NMR (376 MHz, $CDCl_3$): δ = –(132.25–132.32) (2 F) ppm. HRMS: *m*/*z* calcd. for $C_{23}H_{18}BF_2NO_2$ [M^+] 389.1399; found 389.1399.

10-Bromo-6,6-difluoro-13-phenyl-6*H*-benzo[5,6][1,3,2]oxaza-borinino[3,4-*a*]quinolin-5-ium-6-uide (5e): Yellow solid; m.p. 292–294 °C. IR (KBr): $\tilde{\nu}$ = 3093, 3057, 2991, 2366, 1734, 1622, 1593, 1467, 1392, 1354, 1249, 1205, 1101, 1001, 933, 871, 812, 759, 704, 680, 626, 597 cm^{-1}. ^{1}H NMR (400 MHz, $CDCl_3$): δ = 7.04–7.02 (t, *J* = 8.0 Hz, 1 H), 7.48–7.45 (dd, *J* = 16.0, 4.0 Hz, 1 H), 7.67–7.55 (m, 5 H), 7.83–7.79 (t, *J* = 8.0 Hz, 1 H), 7.92 (s, 1 H), 7.95–7.93 (d, *J* = 8.0 Hz, 1 H), 8.07–8.06 (dd, *J* = 4.0 Hz, 1 H), 8.16–8.14 (d, *J* = 8.0 Hz, 1 H) ppm. ^{13}C NMR (100 MHz, $CDCl_3$): δ = 117.4, 120.5, 126.0, 127.1, 127.7, 128.8, 129.0, 129.4, 130.7, 134.7, 155.9 ppm. ^{11}B NMR (128 MHz, $CDCL_3$): δ = 1.51 (s, BF_2) ppm. ^{19}F NMR (376 MHz, $CDCl_3$): δ = –(132.38–132.44) (2 F) ppm.

HRMS: *m*/*z* calcd. for $C_{21}H_{13}BBrF_2NO$ [M^+] 423.0242; found 423.0257.

3-Chloro-6,6-difluoro-13-phenyl-6*H*-benzo[5,6][1,3,2]oxazaborinino[3,4-*a*]quinolin-5-ium-6-uide (5f): Yellow solid; m.p. 240–242 °C. IR (KBr): ṽ = 3136, 3061, 2976, 2339, 1789, 1607, 1598, 1541, 1512, 1263, 1083, 1066, 931, 852, 833, 753, 740, 698, 686, 685 cm^{-1}. ^1H NMR (400 MHz, $CDCl_3$): δ = 7.07–7.03 (t, *J* = 8.0 Hz, 1 H), 7.24–7.22 (d, *J* = 8.0 Hz, 1 H), 7.70–7.53 (m, 8 H), 7.96–7.94 (d, *J* = 8.0 Hz, 1 H), 8.13 (s, 1 H), 9.10–9.01 (m, 1 H) ppm. ^{13}C NMR (100 MHz, $CDCl_3$): δ = 110.6, 110.8, 115.8, 118.4, 120.3, 120.5, 122.0, 122.2, 126.7, 127.8, 127.9, 128.1, 129.1, 129.3, 129.5, 130.1, 135.6, 135.9, 137.6, 151.6, 154.6, 156.2 ppm. ^{11}B NMR (128 MHz, $CDCl_3$): δ = 1.54 (s, BF_2) ppm. ^{19}F NMR (376 MHz, $CDCl_3$): δ = –(132.22–132.16) (2 F) ppm. HRMS: *m*/*z* calcd. for $C_{21}H_{13}BClF_2NO$ [M^+] 379.0747; found 379.0759.

2-Chloro-6,6-difluoro-13-phenyl-6*H*-benzo[5,6][1,3,2]oxazaborinino[3,4-*a*]quinolin-5-ium-6-uide (5g): Yellow solid; m.p. 283–285 °C. IR (KBr): ṽ = 3140, 3082, 3026, 2976, 2339, 1730, 1602, 1546, 1448, 1384, 1263, 1155, 1099, 1078, 1064, 923, 844, 752, 700 cm^{-1}. ^1H NMR (400 MHz, $CDCl_3$): δ = 7.09–7.05 (t, *J* = 8.0 Hz, 1 H), 7.25–7.23 (d, *J* = 8.0 Hz, 1 H), 7.68–7.55 (m, 5 H), 7.87–7.84 (dd, *J* = 16.0, 4.0 Hz, 1 H), 7.93–7.92 (d, *J* = 4.0 Hz, 1 H), 7.97–7.94 (dd, *J* = 16.0, 4.0 Hz, 1 H), 8.13 (s, 1 H), 9.02–9.00 (d, *J* = 8.0 Hz, 1 H) ppm. ^{13}C NMR (100 MHz, $CDCl_3$): δ = 118.5, 120.4, 120.5, 125.5, 126.7, 129.1, 129.3, 130.2, 133.1, 134.2, 135.8, 154.7, 156.2 ppm. ^{11}B NMR (128 MHz, $CDCL_3$): δ = 1.50 (s, BF_2) ppm. ^{19}F NMR (376 MHz, $CDCl_3$): δ = –(132.10–132.03) (2 F) ppm. HRMS: *m*/*z* calcd. for $C_{21}H_{13}BClF_2NO$ [M^+] 379.0747; found 379.0753.

2,6,6-Trifluoro-13-phenyl-6*H*-benzo[5,6][1,3,2]oxazaborinino[3,4-*a*]quinolin-5-ium-6-uide (5h): Yellow solid; m.p. 217–219 °C. IR (KBr): ṽ = 3138, 3084, 3028, 2971, 2364, 1913, 1604, 1587, 1548, 1508, 1492, 1388, 1134, 1097, 1078, 1064, 875, 775, 754, 700 cm^{-1}. ^1H NMR (400 MHz, $CDCl_3$): δ = 7.07–7.03 (t, *J* = 8.0 Hz, 1 H), 7.24–7.22 (d, *J* = 8.0 Hz, 1 H), 7.68–7.41 (m, 7 H), 7.92–7.90 (d, *J* = 8.0 Hz, 1 H), 7.96–7.94 (d, *J* = 4.0 Hz, 1 H), 8.09 (s, 1 H), 9.06–9.04 (d, *J* = 8.0 Hz, 1 H) ppm. ^{13}C NMR (100 MHz, $CDCl_3$): δ = 117.7, 120.4, 120.5, 120.6, 124.4, 126.8, 127.9, 128.0, 128.2, 128.3, 128.7, 128.9, 129.2, 130.1, 135.9, 135.9, 139.4, 155.1, 156.2 ppm. ^{11}B NMR (128 MHz, $CDCL_3$): δ = 1.47 (s, BF_2) ppm. ^{19}F NMR (376 MHz, $CDCl_3$): δ = –(131.99–131.92) (2 F), –(132.54–132.48) (d, *J* = 22.5 Hz, 2 F) ppm. HRMS: *m*/*z* calcd. for $C_{21}H_{13}BF_3NO$ [M^+] 363.1042; found 363.1053.

2-Bromo-6,6-difluoro-13-phenyl-6*H*-benzo[5,6][1,3,2]oxazaborinino[3,4-*a*]quinolin-5-ium-6-uide (5i): Yellow solid; m.p. 256–258 °C. IR (KBr): ṽ = 3140, 3078, 3026, 1948, 1602, 1546, 1448, 1382, 1153, 1107, 1076, 999, 875, 750, 663, 605, 575 cm^{-1}. ^1H NMR (400 MHz, $CDCl_3$): δ = 7.07–7.03 (t, *J* = 8.0 Hz, 1 H), 7.24–7.22 (d, *J* = 8.0 Hz, 1 H), 7.68–7.54 (m, 6 H), 8.00–7.93 (m, 2 H), 8.09–8.08 (d, *J* = 4.0 Hz, 1 H), 8.12 (s, 1 H), 8.94–8.92 (d, *J* = 8.0 Hz, 1 H) ppm. ^{13}C NMR (100 MHz, $CDCl_3$): δ = 115.8, 118.5, 120.3, 120.5, 122.3, 126.7, 126.8, 127.8, 128.8, 129.1, 129.3, 130.2, 135.7, 135.8, 154.2, 156.4 ppm. ^{11}B NMR (128 MHz, $CDCL_3$): δ = 1.49 (s, BF_2) ppm. ^{19}F NMR (376 MHz, $CDCl_3$): δ = –(132.13–132.07) (2 F) ppm. HRMS: *m*/*z* calcd. for $C_{21}H_{13}BBrF_2NO$ [M^+] 423.0242; found 423.0249.

6,6-Difluoro-2-methoxy-13-phenyl-6*H*-benzo[5,6][1,3,2]oxazaborinino[3,4-*a*]quinolin-5-ium-6-uide (5j): Yellow solid; m.p. 231–233 °C. IR (KBr): ṽ = 3057, 3001, 2843, 2700, 2331, 1614, 1600, 1421, 1388, 1253, 1232, 1152, 1020, 999, 970, 898, 883, 756, 698, 524 cm^{-1}. ^1H NMR (400 MHz, $CDCl_3$): δ = 3.89 (s, 3 H), 7.15–7.06 (m, 1 H), 7.33–7.30 (m, 2 H), 7.73–7.50 (m, 6 H), 7.87–7.85 (d, *J* = 8.0 Hz, 1 H), 8.04 (s, 1 H), 8.13–8.11 (d, *J* = 8.0 Hz, 1 H), 8.48–8.46 (d, *J* = 8.0 Hz, 1 H) ppm. ^{13}C NMR (100 MHz, $CDCl_3$): δ = 55.8, 104.8, 118.8, 119.4, 120.6, 126.3, 128.3, 128.9, 129.0, 129.0, 129.1, 129.2, 129.4, 129.9 ppm. ^{11}B NMR (128 MHz, $CDCL_3$): δ = 1.56 (s, BF_2) ppm. ^{19}F NMR (376 MHz, $CDCl_3$): δ = –(132.72) (2 F) ppm. HRMS: *m*/*z* calcd. for $C_{22}H_{16}BF_2NO_2$ [M^+] 375.1242; found 375.1246.

6,6-Difluoro-2-methyl-13-phenyl-6*H*-benzo[5,6][1,3,2]oxazaborinino[3,4-*a*]quinolin-5-ium-6-uide (5k): Yellow solid; m.p. 250–252 °C. IR (KBr): ṽ = 3059, 3026, 2987, 2816, 2361, 1749, 1604, 1552, 1494, 1408, 1386, 1296, 1265, 1132, 1103, 1078, 1008, 937, 752, 704, 613 cm^{-1}. ^1H NMR (400 MHz, $CDCl_3$): δ = 2.52 (s, 3 H), 7.06–7.02 (t, *J* = 8.0 Hz, 1 H), 7.24–7.22 (d, *J* = 8.0 Hz, 1 H), 7.53–7.51 (d, *J* = 8.0 Hz, 1 H), 7.67–7.55 (m, 5 H), 7.70 (s, 1 H), 7.76–7.74 (d, *J* = 8.0 Hz, 1 H),7.96–7.94 (d, *J* = 8.0 Hz, 1 H), 8.06 (s, 1 H), 8.95–8.93 (d, *J* = 8.0 Hz, 1 H) ppm. ^{13}C NMR (100 MHz, $CDCl_3$): δ = 21.5, 117.5, 120.2, 120.3, 124.7, 125.6, 126.6, 126.7, 129.0, 129.2, 129.7, 134.6, 135.1, 136.6, 138.3, 139.2, 150.9, 154.6, 156.1 ppm. ^{11}B NMR (128 MHz, $CDCl_3$): δ = 1.54 (s, BF_2) ppm. ^{19}F NMR (376 MHz, $CDCl_3$): δ = –(132.74–132.68) (2 F) ppm. HRMS: *m*/*z* calcd. for $C_{22}H_{16}BF_2NO$ [M^+] 359.1293; found 359.1298.

6,6-Difluoro-1,3-dimethyl-13-phenyl-6*H*-benzo[5,6][1,3,2]oxazaborinino[3,4-*a*]quinolin-5-ium-6-uide (5l): Yellow solid; m.p. 276–278 °C. IR (KBr): ṽ = 3099, 3053, 3013, 2987, 2346, 1737, 1624, 1604, 1587, 1514, 1446, 1354, 1246, 1101, 1049, 1008, 976, 862, 765, 713, 650, 603 cm^{-1}. ^1H NMR (400 MHz, $CDCl_3$): δ = 2.07 (s, 3 H), 2.66 (s, 3 H), 7.14–7.10 (t, *J* = 8.0 Hz, 1 H), 7.36–7.34 (d, *J* = 8.0 Hz, 1 H), 7.63–7.42 (m, 7 H), 7.96–7.86 (m, 2 H), 8.00 (s, 1 H) ppm. ^{13}C NMR (100 MHz, $CDCl_3$): δ = 21.9, 23.8, 119.3, 119.4, 120.8, 121.9, 123.4, 127.9, 127.9, 128.8, 128.8, 129.2, 129.8, 135.4, 136.0, 137.3, 139.6, 146.9, 157.0, 159.0 ppm. ^{11}B NMR (128 MHz, $CDCl_3$): δ = 0.19–0.15 (d, *J* = 5.1 Hz, BF_2) ppm. ^{19}F NMR (376 MHz, $CDCl_3$): δ = –(150.17.74–150.19) (2 F) ppm. HRMS: *m*/*z* calcd. for $C_{23}H_{18}BF_2NO$ [M^+] 373.1450; found 373.1455.

Acknowledgments

U. B. thanks the Council of Scientific and Industrial Research (CSIR), New Delhi for providing SRF. The DST-FIST NMR facility at VIT University is greatly acknowledged. The authors thank Dr. P. G. Aravindan, Associate Professor, SAS, VIT University, India, for solving the X-ray data. The authors thank Dr. S. Easwaramoorthi, Scientist, CLRI, Chennai, India, for electrochemical studies.

[1] a) L. Yuan, W. Lin, K. Zheng, L. He, W. Huang, *Chem. Soc. Rev.* **2013**, *42*, 622–661; b) H. Kobayashi, M. Ogawa, R. Alford, P. L. Choyke, Y. Urano, *Chem. Rev.* **2009**, *110*, 2620–2640; c) Y. Zhou, Z. Xu, J. Yoon, *Chem. Soc. Rev.* **2011**, *40*, 2222–2235; d) G. Beer, C. Niederalt, S. Grimme, J. Daub, *Angew. Chem. Int. Ed.* **2000**, *39*, 3252–3255; *Angew. Chem.* **2000**, *112*, 3385; e) S. Ertan-Ela, M. D. Yilmaz, B. Icli, Y. Dede, S. Icli, E. U. Akkaya, *Org. Lett.* **2008**, *10*, 3299–3302; f) C. F. A. Gómez-Durán, I. García-Moreno, A. Costela, V. Martin, R. Sastre, J. Bañuelos, F. L. Arbeloa, I. López Arbeloa, E. Peña-Cabrera, *Chem. Commun.* **2010**, *46*, 5103–5105; g) Y. Shirota, M. Kinoshita, T. Noda, K. Okumoto, T. Ohara, *J. Am. Chem. Soc.* **2000**, *122*, 11021–11022; h) C. Chen, *Chem. Mater.* **2004**, *16*, 4389–4400.

[2] a) G. Ulrich, R. Ziessel, A. Harriman, *Angew. Chem. Int. Ed.* **2008**, *47*, 1184–1201; *Angew. Chem.* **2008**, *120*, 1202–1219; b) R. Ziessel, G. Ulrich, A. Harriman, *New J. Chem.* **2007**, *31*,

496–501; c) D. Frath, J. Massue, G. Ulrich, R. Ziessel, *Angew. Chem. Int. Ed.* **2014**, *53*, 2290–2310.
[3] a) P. F. Kaiser, J. M. White, C. A. Hutton, *J. Am. Chem. Soc.* **2008**, *130*, 16450–16451; b) Y. Zhou, S. Chi, X. Qian, *Org. Lett.* **2008**, *10*, 633–636; c) J. Feng, B. Liag, D. Wang, D. Xue, X. Li, *Org. Lett.* **2008**, *10*, 4437; d) Y. Zhou, J. W. Kim, R. Nandhakumar, M. J. Kim, E. Cho, Y. S. Kim, Y. H. Jang, C. Lee, S. Han, K. M. Kim, J.-J. Kim, Y. Yoon, *Chem. Commun.* **2010**, *46*, 6512–6514; e) Y. Qin, C. Pagba, P. Piotrowiak, F. Jakle, *J. Am. Chem. Soc.* **2004**, *126*, 7015–7018; f) F. Cheng, F. Jakle, *Chem. Commun.* **2010**, *46*, 3717–3719.
[4] a) D. Li, K. Wang, S. Huang, S. Qu, X. Liu, Q. Zhu, H. Zhang, Y. Wang, *J. Mater. Chem.* **2011**, *21*, 15298–15304; b) D. Li, H. Zhang, C. Wang, S. Huang, J. Guo, Y. Wang, *J. Mater. Chem.* **2012**, *22*, 4319–4328.
[5] a) J. Yoshino, N. Kano, T. Kawashima, *Chem. Commun.* **2007**, 559–561; b) H. Maeda, Y. Mihashi, Y. Haketa, *Org. Lett.* **2008**, *10*, 3179–3182; c) Y. Kubota, T. Tsuzuki, K. Funabiki, M. Ebihara, M. Matsui, *Org. Lett.* **2010**, *12*, 4010–4013; d) G. Ulrich, R. Ziessel, A. Harriman, *Angew. Chem. Int. Ed.* **2008**, *47*, 1184–1201; *Angew. Chem.* **2008**, *120*, 1202; e) S. Xu, K. Chen, H. Tian, *J. Mater. Chem.* **2005**, *15*, 2676–2680; f) Y. Inokuma##Inokuma, J. H. Kwon, T. K. Ahn, M.-C. Yoo, D. Kim, A. Osuka, *Angew. Chem. Int. Ed.* **2006**, *45*, 958–961; *Angew. Chem.* **2006**, *118*, 972; g) L. Wu, K. Burgess, *J. Am. Chem. Soc.* **2008**, *130*, 4089–4096; h) Y. Zhou, Y. Xiao, S. Chi, X. Qian, *Org. Lett.* **2008**, *10*, 633–636.
[6] a) A. Loudet, K. Burgess, *Chem. Rev.* **2007**, *107*, 4891–4932; b) A. Dvivedi, P. Rajakannu, M. Ravikanth, *Dalton Trans.* **2015**, *44*, 4054–4062; c) K. Tram, H. Yan, H. A. Jenkins, S. Vassiliev, D. Bruce, *Dyes Pigm.* **2009**, *82*, 392–395; d) Z. N. Sun, H. L. Wang, F. Q. Liu, Y. Chen, P. Kwong, H. Tam, D. Yang, *Org. Lett.* **2009**, *11*, 1887–1890; e) M. S. T. Goncalves, *Chem. Rev.* **2009**, *109*, 190–212; f) S. Hattori, K. Ohkubo, Y. Urano, H. Sunahara, T. Nagano, Y. Wada, N. V. Tkachenko, H. Lemmetyinen, S. Fukuzumi, *J. Phys. Chem. B* **2005**, *109*, 15368–15375; g) T. Rousseau, A. Cravino, T. Bura, G. Ulrich, R. Ziessel, J. Roncali, *Chem. Commun.* **2009**, 1673–1675; h) T. Rousseau, A. Cravino, T. Bura, G. Ulrich, R. Ziessel, J. Roncali, *J. Mater. Chem.* **2009**, *19*, 2298–2300; i) S. Ozlem, E. U. Akkaya, *J. Am. Chem. Soc.* **2009**, *131*, 48–49.
[7] a) A. C. Benniston, G. Copley, H. Lemmetyinen, N. V. Tkachenko, *Eur. J. Org. Chem.* **2010**, 2867–2877; b) J. Massue, D. Frath, P. Retailleau, G. Ulrich, R. Ziessel, *Chem. Eur. J.* **2013**, *19*, 5375–5386.
[8] a) D. Zhang, Y. Wen, Y. Xiao, G. Yu, Y. Liu, X. Qian, *Chem. Commun.* **2008**, 4777–4779; b) W. Qin, T. Rohand, M. Baruah, A. Stefan, M. V. Auweraer, W. Dehaen, N. Boens, *Chem. Phys. Lett.* **2006**, *420*, 562–568.
[9] a) F. Ito, T. Nagai, Y. Ono, K. Yamaguchi, H. Furuta, T. Nagamura, *Chem. Phys. Lett.* **2007**, *435*, 283–288; b) S. P. Singh, T. Gayathri, *Eur. J. Org. Chem.* **2014**, 4689–4707.
[10] a) M. Matsui, R. Ikeda, Y. Kubota, K. Funabiki, *Tetrahedron Lett.* **2009**, *50*, 5047–5049; b) Y. Kubota, J. Uehara, K. Funabiki, M. Ebihara, M. Matsui, *Tetrahedron Lett.* **2010**, *51*, 6195–6198; c) T. Ozdemir, S. Atilgan, I. Kutuk, L. T. Yildirim, A. Tulek, M. Bayindir, E. U. Akkaya, *Org. Lett.* **2009**, *11*, 2105–2107; d) Y. Ooyama, S. Nabeshima, T. Mamura, H. E. Ooyama, K. Yoshida, *Tetrahedron* **2010**, *66*, 7954–7960; e) T. K. Khan, P. Sheokand, N. Agarwal, *Eur. J. Org. Chem.* **2014**, 1416–1422.
[11] a) R. Ziessel, G. Ulrich, A. Harriman, *New J. Chem.* **2007**, *31*, 496–501; b) N. Saki, T. Dinc, E. U. Akkaya, *Tetrahedron* **2006**, *62*, 2724–2728.
[12] a) M. Santra, H. Moon, M.-H. Park, T.-W. Lee, Y. K. Kim, K. H. Ahn, *Chem. Eur. J.* **2012**, *18*, 9886–9893; b) J. Massue, D. Frath, G. Ulrich, P. Retailleau, R. Ziessel, *Org. Lett.* **2012**, *14*, 230–233; c) Y. Kubota, T. Tsuzuki, K. Funabiki, M. Ebihara, M. Matsui, *Org. Lett.* **2010**, *12*, 4010–4013; d) Y. Kubota, H. Hara, S. Tanaka, K. Funabiki, M. Matsui, *Org. Lett.* **2011**, *13*, 6544–6547; e) Y. Kubota, S. Tanaka, K. Funabiki, M. Matsu, *Org. Lett.* **2012**, *14*, 4682–4685; f) Y.-Y. Wu, Y. Chen, G.-Z. Gou, W.-H. Mu, X.-J. Lv, M.-L. Du, W.-F. Fu, *Org. Lett.* **2012**, *14*, 5226–5229; g) B. J. Liddle, R. M. Silva, T. J. Morin, F. P. Macedo, R. Shukla, S. V. Lindeman, J. R. Gardinier, *J. Org. Chem.* **2007**, *72*, 5637–5646; h) D. Curiel, M. Mas-Montoya, L. Usea, A. Espinosa, R. A. Orenes, P. Molina, *Org. Lett.* **2012**, *14*, 3360–3363; i) Z. Li, X. Lv, Y. Chen, W.-F. Fu, *Dyes Pigm.* **2014**, *105*, 157–162; j) D. Frath, A. Poirel, G. Ulrich, A. D. Nicola, R. Ziessel, *Chem. Commun.* **2013**, *49*, 4908–4910; k) . Y. Yang, X. Su, C. N. Carroll, I. Aprahamian, *Chem. Sci.* **2012**, *3*, 610–613; l) W. Yan, C. Hong, G. Long, Y. Yang, Z. Liu, Z. Bian, Y. Chen, C. Huang, *Dyes Pigm.* **2014**, *106*, 197–204; m) X. Li, Y.-A. Son, *Dyes Pigm.* **2014**, *107*, 182–187; n) Y. Meesala, V. Kavala, H.-C. Chang, T.-S. Kuo, C.-F. Yao, W.-Z. Lee, *Dalton Trans.* **2015**, *44*, 1120–1129.
[13] R.-Z. Ma, Q.-C. Yao, X. Yang, M. Xia, *J. Fluorine Chem.* **2012**, *137*, 93–98.
[14] W. Li, W. Lin, J. Wang, Z. Guan, *Org. Lett.* **2013**, *15*, 1768–1771.
[15] a) S. Easwaramoorthi, B. Umamahesh, P. Cheranmadevi, R. S. Rathore, K. I. Sathiyanarayanan, *RSC Adv.* **2013**, *3*, 1243–1254; b) M. Vedamalai, S.-P. Wu, *Eur. J. Org. Chem.* **2012**, 1158–1163.
[16] N. Gao, C. Cheng, C. Yu, E. Hao, S. Wang, J. Wang, Y. Wei, X. Mu, L. Jiao, *Dalton Trans.* **2014**, *43*, 7121–7127.

Received: April 10, 2015
Published Online: July 15, 2015

